ceramics

MDPI

Article

Composite Ceramics in the Na_2O–CaO–SiO_2–P_2O_5 System Obtained from Pastes Including Hydroxyapatite and an Aqueous Solution of Sodium Silicate

Maksim Kaimonov [1,*], Tatiana Safronova [1,2], Tatiana Shatalova [1,2], Yaroslav Filippov [1,3], Irina Tikhomirova [4] and Nikollay Sergeev [5]

[1] Department of Materials Science, Lomonosov Moscow State University, Building, 73, Leninskie Gory, 1, 119991 Moscow, Russia
[2] Department of Chemistry, Lomonosov Moscow State University, Building, 3, Leninskie Gory, 1, 119991 Moscow, Russia
[3] Research Institute of Mechanics, Lomonosov Moscow State University, Michurinsky Pr., 1, 119192 Moscow, Russia
[4] Department of General Technology of Silicates, Mendeleev University of Chemical Technology, Building, 1, Geroyev Panfilovtsev, 20, 125480 Moscow, Russia
[5] The Kizhner Research Center, National Research Tomsk Polytechnic University, Building, 2, Lenin Ave, 43a, 634050 Tomsk, Russia
* Correspondence: kaimonovmr@my.msu.ru

Abstract: The new approach to obtaining ceramic materials in the Na_2O–CaO–SiO_2–P_2O_5 system based on the binder—an aqueous solution of sodium silicate and filler—hydroxyapatite was shown in current research. After heat treatment at 500 °C and 700 °C, the ceramic samples included non-reacted hydroxyapatite $Ca_{10}(PO_4)_6(OH)_2$, β-rhenanite β-$NaCaPO_4$ and sodium calcium silicophosphate $Na_2Ca_4(PO_4)_2SiO_4$. An increase in temperature to 900 °C and 1100 °C allowed to obtain ceramic materials with the following phases: devitrite $Na_2Ca_3Si_6O_{16}$, β-rhenanite β-$NaCaPO_4$, β-wollastonite β-$CaSiO_3$, and silicon dioxide SiO_2. The strength of ceramic samples rose with increasing temperature from ≈7.0 MPa (bending) and ≈7.2 MPa (compression) at 500 °C to ≈9.5 MPa (bending) and ≈31.6 MPa (compression) at 1100 °C. At the same time, the apparent density decreased from 1.71 g/cm^3 to 1.15 g/cm^3. The top of the compressive strength equal to 31.6 MPa was observed when the apparent density was 1.15 g/cm^3. Obtained ceramics consisted of biocompatible phases, widely studied in the literature; thus, it confirms the possibility of using an aqueous solution of sodium silicate in medical materials science.

Keywords: hydroxyapatite; aqueous solution of sodium silicate; pastes; pre-ceramic samples; ceramics; composites; Na_2O–CaO–SiO_2–P_2O_5 system

Citation: Kaimonov, M.; Safronova, T.; Shatalova, T.; Filippov, Y.; Tikhomirova, I.; Sergeev, N. Composite Ceramics in the Na_2O–CaO–SiO_2–P_2O_5 System Obtained from Pastes Including Hydroxyapatite and an Aqueous Solution of Sodium Silicate. *Ceramics* **2022**, *5*, 550–561. https://doi.org/10.3390/ceramics5030041

Academic Editors: Margarita A. Goldberg and Elisa Torresani

Received: 30 June 2022
Accepted: 1 September 2022
Published: 5 September 2022

1. Introduction

According to statistics, at least one million operations of bone grafting are performed annually in the world, and these operations rank second in the frequency of tissue transplantation after the transfusion of blood components [1], which stimulates the development of functional medical materials.

Hydroxyapatite (HA) is the most well-known calcium phosphate material that forms the basis of bones and teeth [2] and belongs to second-generation biomaterials [3]. For all time, a large number of studies have been carried out, which showed that in natural hydroxyapatite, the Ca/P molar ratio is not equal to Ca/P ≠ 1.67 but fluctuates in the range of 1.37–1.67 due to the balance between soluble and insoluble phosphate forms [4–6]. Moreover, the mineral phase of bone tissue consists of hydroxyapatite, which contains various supplementary groups and elements [7,8]. Despite this, the similarity between natural and synthetic hydroxyapatite has led to vigorous investigations of the last one as a

biomaterial. Today it is known that synthetic hydroxyapatite is a bioactive material with excellent osteoconductivity. In addition, hydroxyapatite supports adhesion, differentiation, and proliferation of osteoblasts [9]; however, HA is not bioresorbable and does not have high reactivity (the formation of a surface layer of apatite is observed after a month of in vitro tests) [10], plus HA is quite brittle [11]. Nevertheless, it is possible to achieve a rise in the decomposition rate of synthetic hydroxyapatite in biological fluids by increasing the porosity or content of substituting ions in the crystal lattice [9]. Another way to increase resorbability is to fabricate hydroxyapatite–osteoinductive phase composites. Amorphous and (or) crystalline silicate phases of the Na_2O–CaO–SiO_2–P_2O_5 system can act as an osteoinductive phase.

The Na_2O–CaO–SiO_2–P_2O_5 system is known due to the works of Larry Hench on obtaining the material with unique properties—Bioglass 45S5 [12–15]. This material can bind to both soft tissues and bone tissues; moreover, the strength of the interfacial bond between the bone and materials is comparable to or greater than the strength of the host bone [13]. Dissolution products of bioactive glasses enhance the expression of genes that control osteogenesis [14], stimulate angiogenic growth factor and endothelial cell tubules formation, and also provide an antibacterial effect [16], which is necessary for the killing of classical pathogenic bacteria (Staphylococcus aureus ATCC25923, Staphylococcus epidermidis, Escherichia coli ATCC25922) detected during wound healing [17]. All this together provides a higher rate of bone formation in comparison with other inorganic bioceramic materials such as hydroxyapatite [18]. However, despite all the evident advantages, Bioglass 45S5 also has some disadvantages [19]: a relatively fast rate of dissolution and resorption, which negatively affects the balance of natural bone tissue remodeling and, in some cases, can lead to the formation of a gap between a tissue and an implant material; low strength characteristics; cytotoxic effect caused by sodium leached into a culture medium.

When obtaining glass-ceramic materials based on Bioglass 45S5 and hydroxyapatite compositions, the possibility exists to eliminate some disadvantages of each material. Studies have been carried out on such composites [20–26], which found that glass-ceramic materials based on Bioglass 45S5 and hydroxyapatite show excellent results in vitro tests. Nevertheless, it should be noted that the approaches to obtaining Bioglass 45S5, both in the considered works and in general, are based on a traditional method—melt quenching [20,23] or a sol-gel [27]. These approaches are economically costly and multistage, and current trends in manufacturing functional materials for medical purposes require innovative approaches to obtaining efficient and affordable biomaterials.

Application of an aqueous solution of sodium silicate ($Na_2O{\cdot}nSiO_2$) as a binder in the creation of biocompatible ceramic materials based on synthetic calcium phosphate powders in the Na_2O–CaO–SiO_2–P_2O_5 system makes it possible to correspond both the base requirements and modern trends. An aqueous solution of sodium silicate is a highly alkaline solution, manufactured by GOST 13078-81 [28], characterized by a silicate modulus—"n" (the molar ratio of silicon oxide to sodium oxide) and having extensive variations of chemical composition by the silicate modulus. Aqueous solutions of sodium silicates with a silicate modulus $n \leq 3.5$ have good wettability, while the wetting time can be different and largely depend on the viscosity of the solution [29]. These materials are cheap, non-flammable, and available for use in greater volume. Aqueous solutions of sodium silicate are mainly used in the construction industry [30], but their potential is greatly underestimated because sodium silicate solutions can be used in medical materials science. It is noted in [31] that the formation of an apatite layer is observed on sodium silicate glass in SBF tests, and in [32], sodium metasilicate was used as a source of silicate groups to obtain silicon-substituted hydroxyapatite (Si-HA) materials.

Hence, the purpose of the current work consisted of obtaining ceramics in the Na_2O–CaO–SiO_2–P_2O_5 system from pre-ceramic blanks formed from highly concentrated suspensions (pastes) based on synthetic calcium phosphate (hydroxyapatite) and aqueous solution of sodium silicate; and determination the potential of an alternative approach to obtaining biocompatible phases and thus bioceramics.

2. Materials and Methods

2.1. Paste Preparation in the Na_2O–CaO–SiO_2–P_2O_5 System

In this work, pastes were obtained, comprising a dispersion medium—an aqueous solution of sodium silicate (GOST 13078-81, JSC "Salavatsteklo"), and a dispersed phase—calcium phosphate powders, in particular, hydroxyapatite $Ca_{10}(PO_4)_6(OH)_2$ (CAS № 1306-06-5, purum.p.a. $\geq$ 96%, Riedel-de Haen, SigmaAldrich Laborchemikalien, 04238, Lot 70080, Seelze, Germany).

The mass percentage of oxides Na_2O, SiO_2, and H_2O in the initial aqueous solution of sodium silicate (SS_{aq}), possessing a density p = 1.48 g/cm^3 and a silicate modulus $n(SiO_2/Na_2O)$ = 2.87, were calculated in accordance with the methodology set out in GOST 13078-81 [28]. It was equal to ω (Na_2O) = 11.05 wt.%, ω (SiO_2) = 30.7 wt.% and ω (H_2O) = 58.25 wt.% respectively.

The initial reagents were taken in the molar ratio $(Na_2O{\cdot}2.87SiO_2)_{aq}/Ca_{10}(PO_4)_6(OH)_2$ = 3:1 (SS_{aq}/HA) (volumetric load is 22%) so that when these are mixed in an agate mortar, homogeneous plastic molding masses were obtained while maintaining the fluidity of them.

2.2. Preparation of Pre-Ceramic Samples in the Na_2O–CaO–SiO_2–P_2O_5 System

The prepared pastes were placed into silicone molds 30 × 10 × 10 mm in size and kept in the air for 24 h at room temperature. The molded pre-ceramic samples were demolded after a day and heat-treated at 60 °C for 24 h to remove residual moisture. All pre-ceramic samples, after demolded, kept their gained shape.

2.3. Preparation of Ceramic Samples in the Na_2O–CaO–SiO_2–P_2O_5 System

Pre-ceramic samples obtained after molding were heat-treated in the air in a furnace at 500 °C, 700 °C, 900 °C, and 1100 °C with exposure for 2 h; the heating rate of the furnace was 5 °C/min; samples were cooled in the furnace.

2.4. Morphological and Structural Characterization

2.4.1. Structural Characterization

The phase composition of pre-ceramic samples resulting from molding into silicone mold and after heat treatment at 60 °C for a day, as well as ceramic samples after firing at specified temperatures, was investigated by X-ray powder diffraction (XRD) with the diffractometer Rigaku D/Max-2500 with a rotating anode (Tokyo, Japan), a 2Θ angle range of 2–70° with a step of 0.02°, a rate of spectrum registration of 5°/min, CuKα radiation (λ = 1.5406 Å). The phases were determined using the ICDD PDF-2 database [33].

Pre-ceramic and ceramic samples were investigated by scanning electron microscopy (SEM) on an electron microscope LEO SUPRA 50VP (Carl Zeiss, Jena, Germany; autoemission source). The investigation was performed at an accelerating voltage of 20 kV (SE2 detector). The samples were pre-coated with a layer of chromium (up to 20 nm).

Particle size distribution of a commercial HA was investigated by Laser-Particle-Sizer ANALYSETTE-22 MicroTec plus (Fritsch, Idar-Oberstein, Germany).

2.4.2. Thermogravimetric and Mass Spectrometric Analysis

Pre-ceramic samples were investigated by thermal analysis (TA), which was performed on a NETZSCH STA 409 PC Luxx simultaneous thermal analyzer (NETZSCH, Selb, Germany) in the air at a heating rate of 10 °C/min. The sample mass was at least 10 mg, and the temperature range was 40–1000 °C. The composition of the gas phase formed upon decomposition of the samples was determined using a quadrupole mass spectrometer QMS 403C Aëolos (NETZSCH, Selb, Germany) combined with a thermal analyzer NETZSCH STA 409 PC Luxx. The mass spectrum (MS) was recorded for the following m/Z value: 18 (H_2O).

2.4.3. Determination of the Strength Properties

The bending and compressive strengths of the obtained ceramics after heat treatment of the pre-ceramic samples size of 30 × 10 × 10 mm molded from pastes based on the aqueous

solution of sodium silicate $(Na_2O{\cdot}2.87SiO_2)_{aq}$ and hydroxyapatite $Ca_{10}(PO_4)_6(OH)_2$ in the molar ratio $(Na_2O{\cdot}2.87SiO_2)_{aq}/Ca_{10}(PO_4)_6(OH)_2$ = 3:1 were determined using the universal testing machine of the 130 FM PW 500 (VEB Thuringer Industriewerk Rauenstein, Germany) and PGM-100MG4 (OOO "Special Design Bureau Stroypribor", Chelyabinsk, Russia).

3. Results and Discussion

According to the XRD data (Figure 1a) and the SEM data (Figure 2), pre-ceramic samples obtained from pastes after their air drying in molds and subsequent heat treatment at 60 °C for 24 h after demolding consisted of only HA phase $Ca_{10}(PO_4)_6(OH)_2$ (PDF 9-432). It is prompting suggestions that there is no reaction between HA and SS_{aq} at the stage of molding, solidification, and drying. Despite the XRD and SEM data, the techniques applied do not allow us to conclude anything about surface reactions. In addition, the XRD pattern in Figure 1 demonstrates indistinct peaks of the HA phase. It is due to the presence of the SS_{aq} phase $(Na_2O{\cdot}2.87SiO_2)$ that is X-ray amorphous (Figure 1b) and, consequently, contributes to X-ray analysis because its content is more than the HA phase (the molar ratio $(Na_2O{\cdot}2.87SiO_2)_{aq}/Ca_{10}(PO_4)_6(OH)_2$ = 3:1).

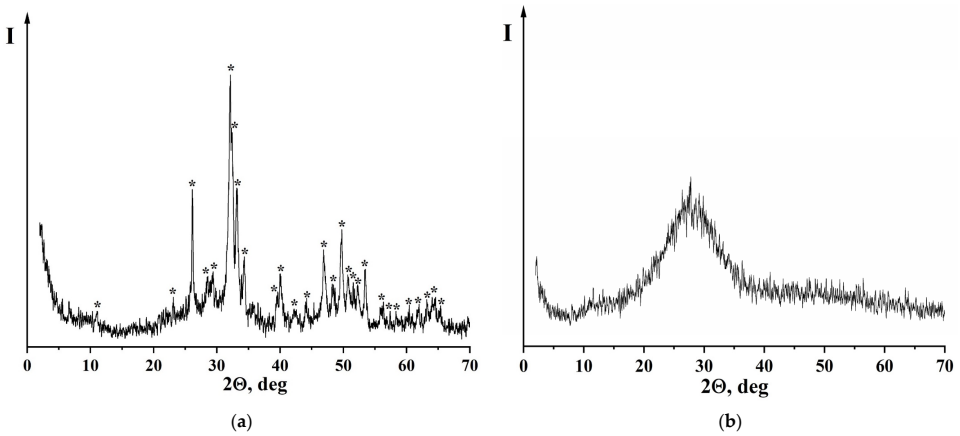

Figure 1. XRD pattern of the pre-ceramic samples obtained from pastes after their air drying in molds and subsequent heat treatment at 60 °C for 24 h: *—$Ca_{10}(PO_4)_6(OH)_2$ (PDF card 9-432) (**a**). XRD pattern of the aqueous solution of sodium silicate after 60 °C with exposure of 24 h (**b**).

The SEM data of pre-ceramic samples show that the particles of HA powder (Figure 2a) after mixing with SS_{aq} and air drying are bounded to each other by a curable mass—amorphous hydrated sodium silicate (Figure 2b). The particle size distribution of a commercial HA is illustrated in Figure 2c. A high level of the specific surface area of HA powder leads to a small count of powder for obtaining homogeneous plastic molding masses with an aqueous solution of sodium silicate while maintaining their fluidity. Hence, as can be expected that, with an increase in the particle size of the calcium phosphate powder, the amount of an aqueous solution of sodium silicate will be required less for bonding particles of a powder to each other and obtaining plastic molding masses. In addition, according to Figure 2, an aqueous solution of sodium silicate with a silicate modulus $n(SiO_2/Na_2O)$ = 2.87 well-wet HA powder. It leads to good adhesion in the hardened state. Following the literature [29], most such hardened compositions on an aqueous solution of sodium silicate fracture cohesively or by a mixed mechanism. It also was marked that composition of HA—SS_{aq} with the molar ratio $(Na_2O{\cdot}2.87SiO_2)_{aq}/Ca_{10}(PO_4)_6(OH)_2$ = 3:1 demonstrates good molding properties. The suspensions were shown well cast into silicon molds in size 30 × 10 × 10 mm with shape preservation after drying (Figure 2d). In prospect, suspensions based on an aqueous solution of sodium silicate with calcium phosphate filler can be used as an extruded material for additive technology, which will be considered in future works. After molding and drying, the volumetric shrinkage of the pre-ceramic samples did not exceed 15%. It depends on the content of SS_{aq} in composition:

the more SS_{aq} content, the more volumetric shrinkage of the samples due to the present water in SS_{aq}.

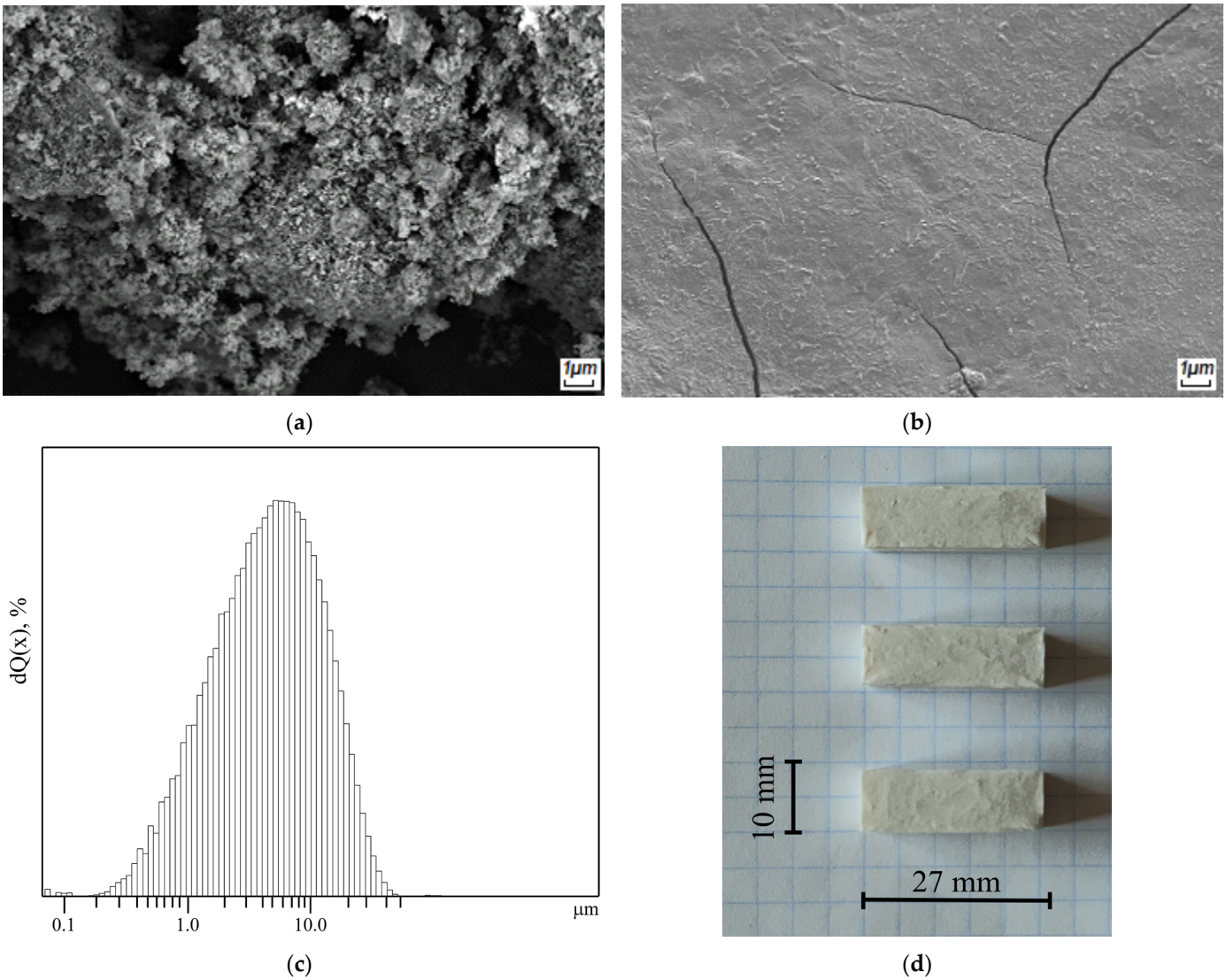

Figure 2. SEM images of the hydroxyapatite powder before (**a**) and after mixing with the aqueous solution of sodium silicate and drying at 60 °C for 24 h (**b**). Particle size distribution of commercial hydroxyapatite (SigmaAldrich) (**c**). Image of the pre-ceramic sample based on the hydroxyapatite powder and the aqueous solution of sodium silicate after demolded and drying at 60 °C for 24 h (**d**).

Thermal analysis of the sample after drying in the air for 24 h at room temperature based on commercial HA and SS_{aq} is shown in Figure 3a. The total mass loss of the sample, when heated from 40 °C to 1000 °C, was about ≈14%.

The mass spectrometry data (Figure 3b) show that the thermal decomposition of the sample is accompanied by the loss of both physically bound water with a maximum of 65 °C and chemically bound water at 200 °C. According to [29], while the temperature rises, the viscosity of a pure aqueous solution of sodium silicate will increase due to the evaporation of moisture, and it makes harden when the water content decrease to 20–30 wt.%. Continuing to heat hydrated sodium silicate above 100–200 °C (depending on the silicate modulus and viscosity) mass loss rate will gradually decrease and turn to zero at about 600 °C when the hydrated forms of silica are completely lost water.

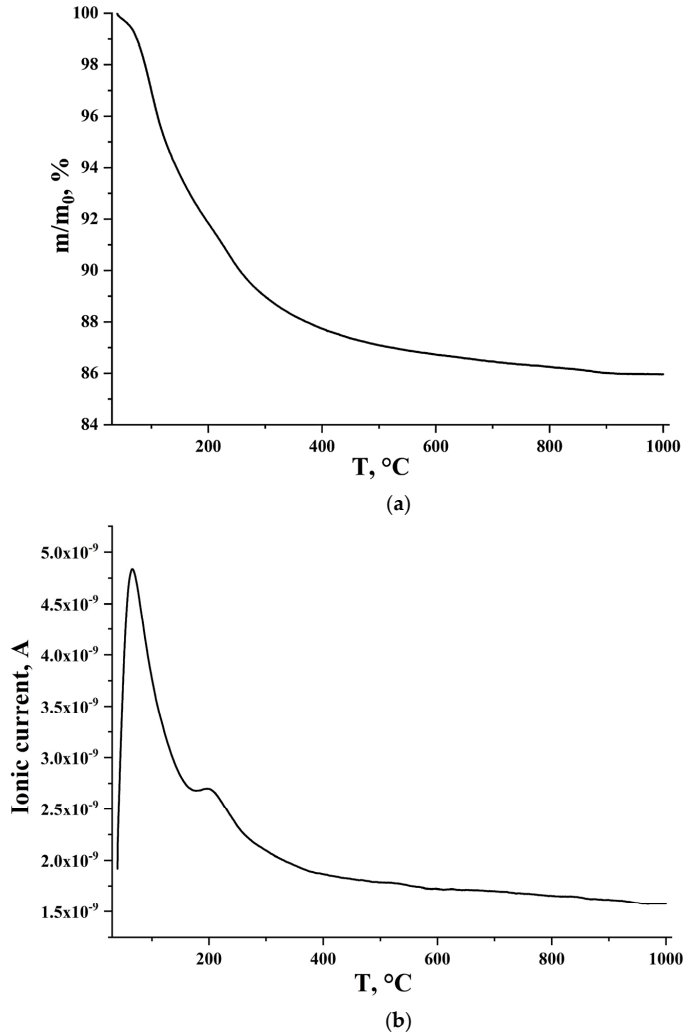

Figure 3. Thermal analysis data (**a**) and Mass spectrum for evolving gas with m/Z (H_2O) = 18 (**b**) of the sample after drying in the air for 24 h at room temperature based on the hydroxyapatite powder and the aqueous solution of sodium silicate.

All the above almost can be wholly attributed to the SS_{aq}-HA system $(Na_2O{\cdot}2.87SiO_2)_{aq}/Ca_{10}(PO_4)_6(OH)_2$. It was suggested earlier in the current work that chemical interaction between SS_{aq} and HA does not occur during molding, solidification, and drying. Plus, the SS_{aq} contains about 58 wt.% water in its composition (ω (H_2O) = 58.25 wt.%), and the molar ratio of SS_{aq} to HA $(Na_2O{\cdot}2.87SiO_2)_{aq}/Ca_{10}(PO_4)_6(OH)_2$ = 3:1. Hence, the base mass loss is due to water loss. Following thermal analysis, this water loss occurs smoothly throughout the entire temperature range from 40 °C to 1000 °C, with amaximum intensity between 40–600 °C. That is consistent with the literature data. Nevertheless, following Figure 3, little mass loss equal to 0.7% exists in the temperature range of 600–1000 °C. It may be related to the presence of interaction products with carbonic acid in compositions during hardening following literature data [34] and their decomposition.

According to [35], after the loss of constitutional water, polymerization of hydrated sodium silicate is observed with the generation of a stable silicon–oxygen framework through covalent-ionic bonds. The modifier cations (Na^+) interaction with the framework is mainly Coulomb. Thus, it can be assumed that at a temperature of about 500 °C, when there is almost no water, chemical interactions between sodium silicate and hydroxyapatite will occur in the composition $(Na_2O{\cdot}2.87SiO_2)/Ca_{10}(PO_4)_6(OH)_2$. That is confirmed by the data of X-ray analysis of fired pre-ceramic samples (Figure 4).

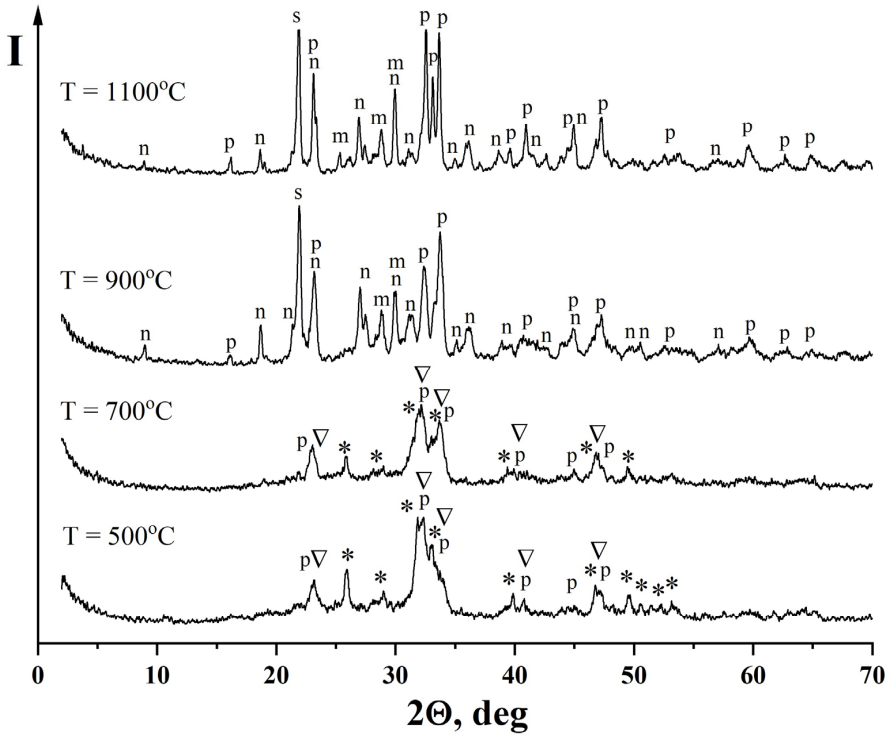

Figure 4. XRD patterns of the ceramic samples obtained from pre-ceramic samples based on the hydroxyapatite powder and the aqueous solution of sodium silicate after heat treatment at 500, 700, 900 and 1100 °C: *—$Ca_{10}(PO_4)_6(OH)_2$, PDF [9-432]; p—$NaCaPO_4$, PDF [29-1193]; ▽—$Na_2Ca_4(PO_4)_2SiO_4$, PDF [32-1053]; n—$Na_2Ca_3Si_6O_{16}$, PDF [23-671]; m—$CaSiO_3$, PDF [27-88]; s—SiO_2, PDF [29-85].

According to the XRD data, the ceramic samples obtained from pre-ceramic samples based on HA $Ca_{10}(PO_4)_6(OH)_2$ and SS_{aq} $(Na_2O{\cdot}2.87SiO_2)_{aq}$, after heat treatment at 500 °C and 700 °C, contained the following phases: non-reacted hydroxyapatite ($Ca_{10}(PO_4)_6(OH)_2$, PDF [9-432]), β-rhenanite (β-$NaCaPO_4$, PDF [29-1193]) and sodium calcium silicophosphate ($Na_2Ca_4(PO_4)_2SiO_4$, PDF [32-1053]). After heat treatment at 900 °C and 1100 °C, the phase composition of ceramics was represented by devitrite ($Na_2Ca_3Si_6O_{16}$, PDF [23-671]), β-rhenanite (β-$NaCaPO_4$, PDF [29-1193]), β-wollastonite (β-$CaSiO_3$, PDF [27-88]) and silicon dioxide (SiO_2, PDF [29-85]) (Table 1).

Table 1. Phase composition of pre-ceramic and ceramic samples.

Pre-Ceramic	500 °C	700 °C	900 °C	1100 °C
$Ca_{10}(PO_4)_6(OH)_2$ Non-identified phase of hydrated $Na_2O{\cdot}2.87SiO_2$	$Ca_{10}(PO_4)_6(OH)_2$ $Na_2Ca_4(PO_4)_2SiO_4$ β-$NaCaPO_4$	$Ca_{10}(PO_4)_6(OH)_2$ $Na_2Ca_4(PO_4)_2SiO_4$ β-$NaCaPO_4$	β-$NaCaPO_4$ $Na_2Ca_3Si_6O_{16}$ β-$CaSiO_3$ SiO_2	β-$NaCaPO_4$ $Na_2Ca_3Si_6O_{16}$ β-$CaSiO_3$ SiO_2

Chemical interactions between sodium silicate and hydroxyapatite can occur in ceramic samples already at 500 °C, which leads to obtaining sodium calcium silicophosphate phase $Na_2Ca_4(PO_4)_2SiO_4$. It crystallizes in the $NaCaPO_4$—Ca_2SiO_4 system with a glaserite-type structure [36]. It should be noted that, as a rule, it is rather laborious to obtain the $Na_2Ca_4(PO_4)_2SiO_4$ phase in its pure form, and, in most cases, that is formed as a secondary phase. Thus, in work [37] during the sintering of hydroxyapatite with bioglass composition (in mol %): 52.6 SiO_2, 25.8 Na_2O, 13.1 CaO, 4.7 P_2O_5, 0.5 Al_2O_3, 3.3 B_2O_3, in the ratio of HA-bioglass equal HA 50 wt.%—bioglass 50 wt.%, it was established that, at 800 °C, the presence of both $Ca_{10}(PO_4)_6(OH)_2$ and $Na_2Ca_4(PO_4)_2SiO_4$ phases were observed, and at 900 °C—$Na_2Ca_4(PO_4)_2SiO_4$ and β-$CaSiO_3$. Moreover, at 900 °C, no HA was present in the

material, indicating a complete reaction. The formation of the $Na_2Ca_4(PO_4)_2SiO_4$ phase as a second phase is also quite often observed during the crystallization of Bioglass 45S5. Thus, in work [38], the following compounds were obtained: $Na_6Ca_3Si_6O_{18}$ (primary) and $Na_2Ca_4(PO_4)_2SiO_4$ (secondary) during crystallization of Bioglass 45S5 in the temperature range of 950–1025 °C. According to the literature data [39,40], such composites are biologically active: they form a surface layer of calcium phosphate in vitro and can directly bind to bone in vivo tests.

Rhenanite $NaCaPO_4$ is a biocompatible phase well-considered in works [41–43]. It is used to produce resorbable inorganic composites [43] for regenerative medicine. Rhenanite can be obtained both in the pure form [44] and by devitrification of bioglasses [45] as a secondary phase.

Further increase in temperature to 900 °C and 1100 °C made it possible to obtain β-wollastonite β-$CaSiO_3$, devitrite $Na_2Ca_3Si_6O_{16}$, and silicon dioxide SiO_2 phases. The absence of hydroxyapatite in composition indicates that the HA completely reacted with sodium silicate. Ceramics based on β-wollastonite β-$CaSiO_3$ has long been known as an osteoconductive material; therefore, chemical reactions on its surface when it is integrated into a bone tissue defect are well investigated in the literature [46,47].

Devitrite $Na_2Ca_3Si_6O_{16}$ belongs to the main elements of Bioglass 45S5; therefore, its presence in the product of a bioglass crystallization is quite much. Thus, devitrite $Na_2Ca_3Si_6O_{16}$ is formed together with the combeite $Na_2Ca_2Si_3O_9$ crystalline phase during Bioglass 45S5 crystallization at 600 °C [48]. In work [49], together with β-wollastonite β-$CaSiO_3$, devitrite $Na_2Ca_3Si_6O_{16}$ was obtained as a result of glass crystallization at 870 °C and 1000 °C, which were prepared by melting a mixture of high purity silica oxides (SiO_2), carbonates from eggshell ($CaCO_3$), and sodium carbonate ($NaCO_3$) at 1500 °C for 1 h and then quenched in the air. In vitro studies show the bioactivity of composites containing the devitrite phase $Na_2Ca_3Si_6O_{16}$ [48–50].

A human body cannot do without silicon and its compounds. In the early stages of osteogenesis, the high content of silicon in a new bone allows an increase in the degree of calcification, while a deficiency of silicon may be a cause of bone distortion [51]. The works [52,53] illustrated silicon dioxide is a biocompatible inorganic material widely used in medicine. In work [54], an animal experiment has shown that silicon is increased the rate of bone mineralization and calcification, similarly to vitamin D [55,56].

It is worth noting that the sodium calcium silicate crystalline phases considered above were obtained in the above research by devitrification compositions based on Bioglass 45S5 and their like. In studies, the bioglasses were obtained either by the traditional method—melt quenching or by a sol-gel. Both methods are energy-intensive, and the whole process of manufacturing sodium calcium silicate crystalline phases is quite laborious.

This paper is considered an alternative and simple enough method for obtaining ceramic materials from pre-ceramic blanks based on an aqueous solution of sodium silicate and a calcium phosphate powder. The ceramic materials considered in the current work, after heat treatment at 500 °C, 700 °C, 900 °C, and 1100 °C, consist of biocompatible phases studied in the literature. It, in turn, confirms the possibility of obtaining bioceramics based on an aqueous solution of sodium silicate and calcium phosphate filler. For providing good biocompatibility properties of the material, both in vitro and in vivo tests, the defined phase composition of bioceramics should be manufactured by varying the ratio of the initial reagents SS_{aq} and HA, replacing HA with another calcium phosphate filler, or adding corrective components.

Micrographs of ceramics obtained from pre-ceramic samples based on $Ca_{10}(PO_4)_6(OH)_2$ and $Na_2O{\cdot}2.87SiO_2$ after heat treatment at 700 °C and 1100 °C are presented in Figure 5.

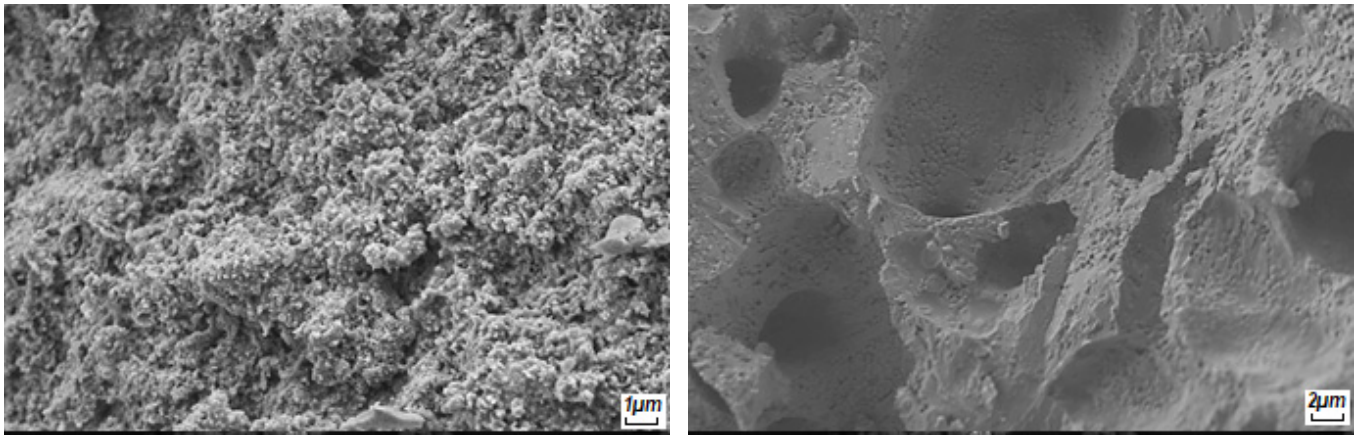

(**a**) (**b**)

Figure 5. SEM images of the ceramic samples obtained from pre-ceramic samples based on the hydroxyapatite powder and the aqueous solution of sodium silicate after heat treatment at 700 °C (**a**) and 1100 °C (**b**).

Following SEM data, the morphology of ceramic samples after heat treatment at 700 °C and 1100 °C (Figure 5a,b) differs from the morphology of pre-ceramic samples (Figure 2b). At 700 °C, a granular structure was observed with an average particle size of 150–250 nm. After heat treatment of a pre-ceramic sample at 1100 °C, the average grain size in a ceramic increased to 250–650 nm, and sintering was observed.

Pre-ceramic samples before firing consist of only two phases: HA and X-ray amorphous SS_{aq}. It is suggested the phase of X-ray amorphous SS_{aq}, when heated, gradually softens and becomes viscous melt. Hence, chemical interaction may occur between melt and filler particles of HA and proceed predominantly through the liquid phase sintering mechanism in the earlier stages. Since fine particles of the sintering material are more soluble in the melt than large ones, then the interaction of the melt with particles of a solid phase leads to their redistribution in size, which is expressed in the coarsening of the average grain sizes of a solid phase. With the rising temperature, the chemical interaction mechanism may change as new compounds are formed. However, in the current work, it was considered only an approach to obtaining bioceramics based on an aqueous solution of sodium silicate and hydroxyapatite without exploring the sintering mechanism.

The mechanical characteristics of the obtained ceramics from pre-ceramic samples after firing at different temperatures are shown in Figure 6a. With increasing temperature, slight growth in bending strength is observed from 7.0 MPa at 500 °C to 9.5 MPa at 1100 °C. At the same time, the compressive strength increases exponentially from 7.2 MPa at 500 °C to 31.6 MPa at 1100 °C. While the mechanical resistance increased, the apparent density decreased (Figure 6b). The top of the compressive strength was observed when the apparent density was 1.15 g/cm^3. Such a set of compressive resistance and apparent density may be associated with the phase composition formation as the temperature increases. At 500 °C, chemical interaction between hydrated sodium silicate and hydroxyapatite begins (Figure 4) with the development of new phases. At 1100 °C, the phase formation process presumably ends, which explains the increase in compressive strength. The amount of the apparent density may also depend on the evaporation of water that leads to the rise of porosity with increasing temperature.

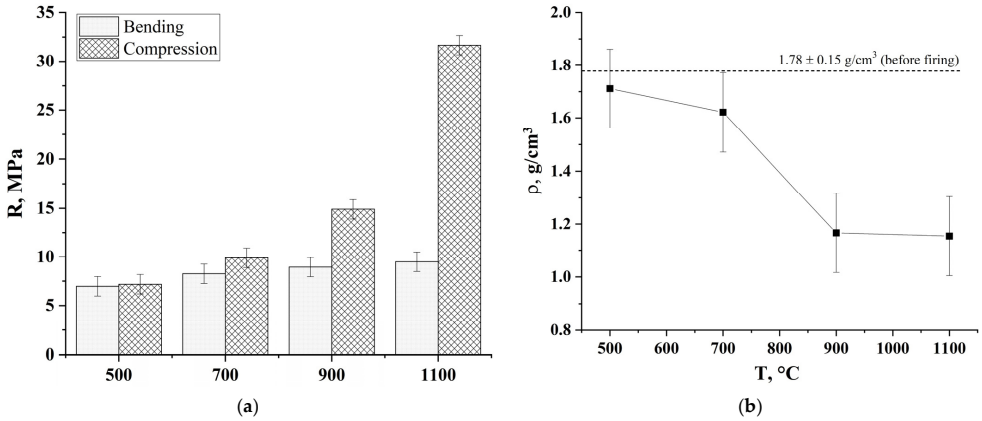

Figure 6. Compressive and bending strengths of the ceramics obtained from pre-ceramic samples based on the hydroxyapatite powder and the aqueous solution of sodium silicate (**a**) and apparent density of ceramics (**b**) after heat treatment at 500, 700, 900 and 1100 °C.

4. Conclusions

The work demonstrates an alternative method for obtaining a ceramic material in the Na_2O–CaO–SiO_2–P_2O_5 system using an aqueous solution of sodium silicate and calcium phosphate filler—hydroxyapatite. The ceramics obtained from pre-ceramic samples after heat treatment at 500, 700, 900, and 1100 °C included the biocompatible phases investigated in the literature. Biocompatible compounds presented in ceramics confirm the possibility of using an aqueous solution of sodium silicate in medical materials science. That approach to manufacturing bioceramics in the Na_2O–CaO–SiO_2–P_2O_5 system does not require producing bioglass by melt quenching or sol-gel followed by crushing and grinding to particle sizes of the order of 60 microns to obtain glass ceramics. Opposite, the new approach makes it possible to obtain a ceramic material immediately after firing hardened pastes based on an aqueous solution of sodium silicate and calcium phosphate powder.

Author Contributions: Conceptualization, M.K.; methodology, M.K.; investigation, M.K., T.S. (Tatiana Safronova), T.S. (Tatiana Shatalova), Y.F., I.T., N.S.; writing—original draft preparation, M.K.; writing—review and editing, M.K.; visualization, M.K., T.S. (Tatiana Safronova), T.S. (Tatiana Shatalova), Y.F., I.T., N.S.; supervision, T.S. (Tatiana Safronova); project administration, T.S. (Tatiana Safronova); funding acquisition, T.S. (Tatiana Safronova). All authors have read and agreed to the published version of the manuscript.

Funding: This work was carried out with financial support from the Russian Foundation for Basic Research (RFBR) (grants No. 20-03-00550 A).

Institutional Review Board Statement: Not applicable.

Informed Consent Statement: Not applicable.

Data Availability Statement: Not applicable.

Acknowledgments: The research was carried out using the equipment of MSU Shared Research Equipment Center "Technologies for obtaining new nanostructured materials and their complex study" and purchased by MSU in the frame of the Equipment Renovation Program (National Project "Science") and in the frame of the MSU Program of Development.

Conflicts of Interest: The authors declare no conflict of interest.

References

1. Aganesov, A.G.; KHeilo, A.L.; Mikaelian, K.P.; Galian, T.N.; Postnikov, Y.V. Long-Term Results of Treatment of Patients with Fractures of Cervical Spine Vertebrare with the Use of Coral-Based Bone Substitute Material BONEMEDIK-S. *Bull. Natl. Med. Surg. Center. N.I. Pirogov.* **2015**, *10*, 41–44.
2. Abdul Halim, N.A.; Hussein, M.Z.; Kandar, M.K. Nanomaterials-Upconverted Hydroxyapatite for Bone Tissue Engineering and a Platform for Drug Delivery. *Int. J. Nanomed.* **2021**, *16*, 6477–6496. [CrossRef]

3. Ievlev, V.M.; Putlyaev, V.I.; Safronova, T.V.; Evdokimov, P.V. Additive Technologies for Making Highly Permeable Inorganic Materials with Tailored Morphological Architectonics for Medicine. *Inorg. Mater.* **2015**, *51*, 1297–1315. [CrossRef]
4. Lemesheva, S.A.; Golovanova, O.A.; Turenkov, S.V. Study of the Composition of Human Bone Tissues. *Chem. Sustain. Dev.* **2009**, *17*, 327–332.
5. Tretyakov, Y.D. *Inorganic Chemistry: Chemistry of Intransitive Elements*; Academy: Moscow, Russia, 2004; Volume 2.
6. Putlyaev, V.I. Modern Bioceramic Materials. *Soros Educ. J.* **2004**, *8*, 44–50.
7. Morgan, E.F.; Gerstenfeld, L.C. The Bone Organ System: Form and Function. In *Marcus and Feldman's Osteoporosis*, 5th ed.; Dempster, D.W., Cauley, J.A., Bouxsein, M.L., Cosman, F., Eds.; Academic Press: New York, NY, USA, 2021; Volume 1, pp. 15–35. ISBN 9780128130735.
8. Boanini, E.; Gazzano, M.; Bigi, A. Ionic Substitutions in Calcium Phosphates Synthesized at Low Temperature. *Acta Biomater.* **2010**, *6*, 1882–1894. [CrossRef]
9. Hoppe, A.; Güldal, N.S.; Boccaccini, A.R. A Review of the Biological Response to Ionic Dissolution Products from Bioactive Glasses and Glass-Ceramics. *Biomaterials* **2011**, *32*, 2757–2774. [CrossRef]
10. Fiume, E.; Magnaterra, G.; Rahdar, A.; Verné, E.; Baino, F. Hydroxyapatite for Biomedical Applications: A Short Overview. *Ceramics* **2021**, *4*, 542–563. [CrossRef]
11. Shi, H.; Zhou, Z.; Li, W.; Fan, Y.; Li, Z.; Wei, J. Hydroxyapatite Based Materials for Bone Tissue Engineering: A Brief and Comprehensive Introduction. *Crystals* **2021**, *11*, 149. [CrossRef]
12. Hench, L.L. Bioceramics: From Concept to Clinic. *J. Am. Ceram. Soc.* **1991**, *74*, 1487–1510. [CrossRef]
13. Hench, L.L. The Story of Bioglass®. *J. Mater. Sci. Mater. Med.* **2006**, *17*, 967–978. [CrossRef] [PubMed]
14. Hench, L.L. Genetic Design of Bioactive Glass. *J. Eur. Ceram. Soc.* **2009**, *29*, 1257–1265. [CrossRef]
15. Hench, L.L. Chronology of Bioactive Glass Development and Clinical Applications. *New J. Glass Ceram.* **2013**, *3*, 67–73. [CrossRef]
16. Kaur, G.; Kumar, V.; Pickrell, G.R.; Mauro, J.C.; Lin, Y.; Arya, S.K. Bioactive Glasses in Gene Regulation and Proliferation. In *Biomedical, Therapeutic and Clinical Applications of Bioactive Glasses*; Elsevier: Amsterdam, The Netherlands, 2019; pp. 175–200.
17. Hu, S.; Chang, J.; Liu, M.; Ning, C. Study on Antibacterial Effect of 45S5 Bioglass®. *J. Mater. Sci. Mater. Med.* **2008**, *20*, 281–286. [CrossRef]
18. Ghosh, S.K.; Nandi, S.K.; Kundu, B.; Datta, S.; De, D.K.; Roy, S.K.; Basu, D. In Vivo Response of Porous Hydroxyapatite and β-Tricalcium Phosphate Prepared by Aqueous Solution Combustion Method and Comparison with Bioglass Scaffolds. *J. Biomed. Mater. Res. Part B Appl. Biomater.* **2008**, *86B*, 217–227. [CrossRef]
19. Kansal, I.; Reddy, A.; Muñoz, F.; Choi, S.J.; Kim, H.W.; Tulyaganov, D.U.; Ferreira, J.M.F. Structure, Biodegradation Behavior and Cytotoxicity of Alkali-Containing Alkaline-Earth Phosphosilicate Glasses. *Mater. Sci. Eng. C* **2014**, *44*, 159–165. [CrossRef]
20. Bellucci, D.; Sola, A.; Gazzarri, M.; Chiellini, F.; Cannillo, V. A New Hydroxyapatite-Based Biocomposite for Bone Replacement. *Mater. Sci. Eng. C* **2013**, *33*, 1091–1101. [CrossRef]
21. Demirkiran, H.; Mohandas, A.; Dohi, M.; Fuentes, A.; Nguyen, K.; Aswath, P. Bioactivity and Mineralization of Hydroxyapatite with Bioglass as Sintering Aid and Bioceramics with $Na_3Ca_6(PO_4)_5$ and $Ca_5(PO_4)_2SiO_4$ in a Silicate Matrix. *Mater. Sci. Eng. C* **2010**, *30*, 263–272. [CrossRef]
22. Bellucci, D.; Sola, A.; Cannillo, V. Hydroxyapatite and Tricalcium Phosphate Composites with Bioactive Glass as Second Phase: State of the Art and Current Applications. *J. Biomed. Mater. Res. Part A* **2016**, *104*, 1030–1056. [CrossRef]
23. Goller, G.; Demirkiran, H.; Oktar, F.N.; Demirkesen, E. Processing and Characterization of Bioglass Reinforced Hydroxyapatite Composites. *Ceram. Int.* **2003**, *29*, 721–724. [CrossRef]
24. Rizwan, M.; Hamdi, M.; Basirun, W.J. Bioglass®45S5-Based Composites for Bone Tissue Engineering and Functional Applications. *J. Biomed. Mater. Res. Part A* **2017**, *105*, 3197–3223. [CrossRef]
25. Rizwan, M.; Hamdi, M.; Basirun, W.J.; Kondoh, K.; Umeda, J. Low Pressure Spark Plasma Sintered Hydroxyapatite and Bioglass®Composite Scaffolds for Bone Tissue Repair. *Ceram. Int.* **2018**, *44*, 23052–23062. [CrossRef]
26. Meng, Y.; Qiang, W.; Pang, J. Fabrication and Microstructure of Laminated HAP–45S5 Bioglass Ceramics by Spark Plasma Sintering. *Materials* **2019**, *12*, 484. [CrossRef] [PubMed]
27. Jones, J.R. Review of Bioactive Glass: From Hench to Hybrids. *Acta Biomater.* **2013**, *9*, 4457–4486. [CrossRef] [PubMed]
28. *GOST 13078-81*; Liquid Sodium Glass. Specifications (with Changes N 1, 2). Publishing House of Standards: Moscow, Russia, 1989; p. 14.
29. Korneev, V.I.; Danilov, V.V. *Soluble and Liquid Glass*; St. Petersburg Stroy-izdat: St. Petersburg, Russia, 1996.
30. Alimov, L.A.; Voronin, V.V. *Constructional Materials*; Academy: Moscow, Russia, 2012; ISBN 978-5-7695-8336-0.
31. Takadama, H.; Kim, H.M.; Kokubo, T.; Nakamura, T. Mechanism of Biomineralization of Apatite on a Sodium Silicate Glass: TEM−EDX Study In Vitro. *Chem. Mater.* **2001**, *13*, 1108–1113. [CrossRef]
32. Golovanova, O.A.; Zaits, A.V. Biomimetic Coating of a Titanium Substrate with Silicon-Substituted Hydroxyapatite. *Inorg. Mater.* **2018**, *54*, 1124–1130. [CrossRef]
33. ICDD. *PDF-4+ 2010 (Database)*; Kabekkodu, S., Ed.; International Centre for Diffraction Data: Newtown Square, PA, USA, 2010; Available online: https://www.icdd.com/pdf-2/ (accessed on 7 May 2022).
34. Medvedev, E.F.; Komarevskaya, A.S. IR Spectroscopic Study of the Phase Composition for Sodium Silicate Synthesized in Aqueous Medium. *Glass Ceram.* **2007**, *64*, 7–11. [CrossRef]
35. Greaves, G.N.; Sen, S. Inorganic Glasses, Glass-Forming Liquids and Amorphizing Solids. *Adv. Phys.* **2007**, *56*, 1–166. [CrossRef]

36. COUSIN, O.; RIVENET, M.; BOIVIN, J.C.; ABRAHAM, F. A REFRACTORY BONDING PHASE FUNDAMENTAL STUDY IN THE Na_2O–CaO–P_2O_5–SiO_2 SYSTEM. *Phosphorus Res. Bull.* **1999**, *10*, 183–188. [CrossRef]
37. Tancred, D.C.; Carr, A.J.; McCormack, B.A.O. The Sintering and Mechanical Behavior of Hydroxyapatite with Bioglass Additions. *J. Mater. Sci. Mater. Med.* **2001**, *12*, 81–93. [CrossRef]
38. Aguilar-Reyes, E.A.; Leon-Patino, C.A.; Jacinto-Diaz, B.; Lefebvre, L.P. Mechanical and Microstructural Characterization of 45S5 Bioglass®Scaffolds for Tissue Engineering. In *Biomaterials Science: Processing, Properties and Applications II*; John Wiley & Sons: Hoboken, NJ, USA, 2012; Volume 237, pp. 1–10.
39. Chitra, S.; Bargavi, P.; Durgalakshmi, D.; Rajashree, P.; Balakumar, S. Role of Sintering Temperature Dependent Crystallization of Bioactiveglasses on Erythrocyte and Cytocompatibility. *Processing Appl. Ceram.* **2019**, *13*, 12–23. [CrossRef]
40. Boccaccini, A.R.; Chen, Q.; Lefebvre, L.; Gremillard, L.; Chevalier, J. Sintering, Crystallisation and Biodegradation Behaviour of Bioglass®-Derived Glass–Ceramics. *Faraday Discuss.* **2007**, *136*, 27. [CrossRef] [PubMed]
41. Jalota, S.; Bhaduri, S.B.; Tas, A.C. A New Rhenanite (β-$NaCaPO_4$) and Hydroxyapatite Biphasic Biomaterial for Skeletal Repair. *J. Biomed. Mater. Res. Part B Appl. Biomater.* **2007**, *80B*, 304–316. [CrossRef] [PubMed]
42. Safronova, T.V.; Putlyayev, V.I.; Knotko, A.V.; Filippov, Y.Y.; Klimashina, E.S.; Ryzhov, A.P.; Saidzhonov, B.M. Powder Mixtures Based on Calcium Hydroxyapatite and Sodium Salts. *Inorg. Mater. Appl. Res.* **2018**, *9*, 726–731. [CrossRef]
43. Safronova, T.V. Inorganic Materials for Regenerative Medicine. *Inorg. Mater.* **2021**, *57*, 443–474. [CrossRef]
44. Safronova, T.V.; Putlyaev, V.I.; Steklov, M.Y.; Tretyakov, Y.D. Method for Obtaining a Ceramic Biodegradable Material Based on Rhenanite 2009. Patent RU 2362538 C2, 2009.
45. Vuong, B.X.; Thy, N.N. A Quick Sol-Gel Process to Elaborate a High Bioactive Ceramic Powder. *J. Sci. Technol.* **2015**, *6*, 100–103.
46. de Almeida, M.S.; de Oliveira Fernandes, G.V.; de Oliveira, A.M.; Granjeiro, J.M. Calcium Silicate as a Graft Material for Bone Fractures: A Systematic Review. *J. Int. Med. Res.* **2018**, *46*, 2537–2548. [CrossRef]
47. Núñez-Rodríguez, L.A.; Encinas-Romero, M.A.; Gómez-Álvarez, A.; Valenzuela-García, J.L.; Tiburcio-Munive, G.C. Evaluation of Bioactive Properties of α and β Wollastonite Bioceramics Soaked in a Simulated Body Fluid. *J. Biomater. Nanobiotechnology* **2018**, *9*, 263–276. [CrossRef]
48. Chitra, S.; Bargavi, P.; Durgalakshmi, D.; Rajashree, P.; Balakumar, S. On the Investigation of Structural and Biological Properties of 45S5 Bioglass and β-Tricalcium Phosphate Nanostructured Materials. In Proceedings of the AIP Conference Proceedings, Hisar, India, 18–22 December 2018; AIP Publishing LLC: Melville, NY, USA, 2019; Volume 2115, p. 030242.
49. Ayawanna, J.; Kingnoi, N.; Wanpen, T. Porous Glass-Ceramic Orbital Implants from Egg Shell. *Microsc. Microanal. Res. J. Microsc. Soc. Thail.* **2020**, *33*, 4–8. [CrossRef]
50. Durgalakshmi, D.; Balakumar, S. Nano-Bioglass (NBG) for Bone Regeneration Applications-Preparation and Its Characterization. In Proceedings of the AIP Conference Proceedings, Bombay, India, 3–7 December 2012; American Institute of PhysicsAIP: Hauppauge, NY, USA, 2013; Volume 1512, pp. 122–123.
51. Carlisle, E.M. Silicon: A Requirement in Bone Formation Independent of Vitamin D1. *Calcif. Tissue Int.* **1981**, *33*, 27–34. [CrossRef] [PubMed]
52. Catauro, M.; Bollino, F.; Papale, F. Synthesis of SiO_2 System via Sol–Gel Process: Biocompatibility Tests with a Fibroblast Strain and Release Kinetics. *J. Biomed. Mater. Res. Part A* **2014**, *102*, 1677–1680. [CrossRef] [PubMed]
53. Catauro, M.; Bollino, F.; Papale, F.; Gallicchio, M.; Pacifico, S. Influence of the Polymer Amount on Bioactivity and Biocompatibility of SiO_2/PEG Hybrid Materials Synthesized by Sol–Gel Technique. *Mater. Sci. Eng. C* **2015**, *48*, 548–555. [CrossRef] [PubMed]
54. Vapirov, V.V.; Feoktistov, V.M.; Venskovich, A.A.; Vapirova, N.V. On Silicon's Behavior and Its Biological Role In Nature. *Sci. Notes Petrozavodsk. State Univ.* **2017**, *2*, 95–102.
55. Carlisle, E.M. A Relationship between Silicon and Calcium in Bone Formation. *Fed. Proc.* **1970**, *29*, 565.
56. Carlisle, E.M. Silicon: An Essential Element for the Chick. *Science* **1972**, *178*, 619–621. [CrossRef]